Catalysis Science & Technology

ROYAL SOCIETY OF CHEMISTRY

PAPER

View Article Online
View Journal | View Issue

Cite this: *Catal. Sci. Technol.*, 2024, 14, 293

Controlling dual-positively charged pyrazolium ionic liquids for efficient catalytic conversion of CO_2 into carbonates under mild conditions†

Jean Damascene Ndayambaje,[ab] Irfan Shabbir,[ab] Qianmeng Zhao,[ab] Li Dong,[a] Qian Su *[a] and Weiguo Cheng *[a]

Received 3rd October 2023,
Accepted 2nd December 2023

DOI: 10.1039/d3cy01376f

rsc.li/catalysis

To address the ongoing rise in carbon dioxide (CO_2) emissions, CO_2 utilization presents a promising approach due to its ability to convert CO_2 into valuable industrial products and enable carbon recycling. For this reason, a high-quality catalyst is required to ensure the effective activation and conversion of CO_2. In this study, a series of dicationic pyrazolium ionic liquids (DPzILs) were first synthesized *via* a one-step process and employed as catalysts in the cycloaddition reaction of CO_2 and epoxides, yielding cyclic carbonates. Among the synthesized DPzILs, [DMPz-6]I_2 exhibited outstanding catalytic performance on diluted CO_2 from simulated flue gas (60% CO_2 in N_2), achieving 94.1% PC yield and 100% selectivity under reaction conditions (100 °C and 10 bar CO_2 pressure) without metal, co-catalyst, or solvent. The study investigated the effects of DPzILs structures, catalyst dosage, CO_2 pressure, reaction temperature, and reaction time on the production of cyclic carbonates. Furthermore, [DMPz-6]I_2 could be efficiently recovered and reused seven times without significant degradation of catalytic activity. It demonstrated significant adaptability to various epoxides. Structure–activity studies indicated that PO activation is synergistically facilitated by the presence of C3/C5 hydrogen from dual-pyrazolium cation rings tethered by alkyl chain lengths and a paired halide anion (I^-/Br^-/Cl^-) in DPzILs. Finally, the reaction mechanism was investigated using FT-IR, ^{1}H NMR, and DFT calculations.

1. Introduction

Industrialization and human dependence on non-renewable resources have increased carbon dioxide (CO_2) emissions in the atmosphere. This has intensified the greenhouse effect, causing global warming and environmental damage. Two main strategies have been used to address this issue thus far: carbon dioxide capture and storage[1] and the conversion of CO_2 into beneficial chemical compounds.[2–4] Both tactics view CO_2 as a non-toxic, natural, renewable, abundant, nonflammable resource and low-cost C1 building block.[5] The latter approach converts CO_2 into useful chemicals such carboxylic acid, methane, methanol, urea synthesis, hydrocarbons, and cyclic carbonates.[6–9] The coupling reaction between CO_2 and epoxides that produces cyclic carbonate (Scheme 1) offers several benefits, including 100% atom economy, inexpensive raw materials, negligible byproducts, and environmental friendliness.[10,11] Cyclic carbonates are chemical intermediates synthesized for various fundamental and industrial purposes. They are used as industrial raw materials, monomers for polycarbonates and polyurethanes, electrolytes for secondary lithium batteries, pesticides, cosmetics, paints, pharmaceutical and fine chemical intermediates, and aprotic polar solvents.[12–15]

Over the past two decades, numerous catalysts have been developed to facilitate the cycloaddition of CO_2 with epoxides, leading to the formation of cyclic carbonates. These catalysts include organocatalysts,[16,17] metal-containing catalysts,[18,19] modified molecular sieves,[20,21] non-metal-based catalysts,[22] ionic liquids (ILs), and others.[23–27] Nevertheless,

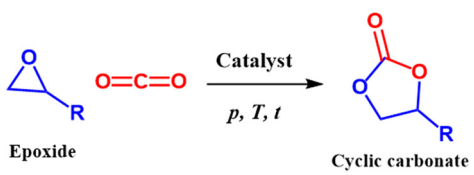

Scheme 1 Cycloaddition of CO_2 with epoxides to form cyclic carbonates.

[a] CAS Key Laboratory of Green Process and Engineering, State Key Laboratory of Multiphase Complex Systems, Beijing Key Laboratory of Ionic Liquids Clean Process, Institute of Process Engineering, Chinese Academy of Sciences, Beijing 100190, P. R. China. E-mail: wgcheng@ipe.ac.cn, qsu@ipe.ac.cn
[b] University of Chinese Academy of Sciences, Beijing 100049, P. R. China

† Electronic supplementary information (ESI) available: Additional experimental procedures and detailed characterization data (1H/13C NMR, ESI-MS, FT-IR spectra, TGA curves, and elemental analysis results), and optimized geometries for the reactants and DPzILs. See DOI: https://doi.org/10.1039/d3cy01376f

certain catalysts require co-catalysts, metals, and organic solvents, as well as challenging reaction conditions. ILs are promising catalysts for CO_2 fixation because of their tunable properties, catalytic activity, and thermal stability.[28,29] Moreover, practically-single-component ILs still face substantial challenges in adjusting the reaction conditions.

Imidazolium-based ionic liquids often demonstrate higher catalytic performance due to their unique properties, including lower viscosity, higher thermal stability, and tunability of physical and chemical properties through structural modification, owing to their five-membered ring.[30,31] Numerous imidazolium-based ILs, including protic, hydroxyl, carboxylic, amino, and dicationic ILs, have been documented to display superior catalytic activity.[32,33] Pyrazolium ionic liquids (PzILs) with a similar ring structure may exhibit comparable catalytic efficacy in CO_2 conversion to cyclic carbonates. Several studies have been conducted in this area. Recently, researchers have reported on dialkyl,[32] protic,[34] hydroxyl,[35] and amino-functionalized[36] pyrazolium ILs and their catalytic activity. The efficiency of these PzILs is comparable to that of imidazolium ILs.[37] However, the modifiability of such PzILs is limited by the single-centered anion–cation pair.

Dicationic ionic liquids (DILs), a subset of the ILs category, have two cationic heads coupled by an aliphatic or aromatic linker and two counteranions.[38] Additionally, their solubility, electrochemical behavior, and thermal stability can be adjusted by modifying the cation, anion, and linker.[39] DILs typically demonstrate higher catalytic activity than monoionic ILs due to multiple factors, such as a higher concentration of active sites, higher charge density, lower viscosity, and improved thermal stability.[40] These properties make DILs a highly effective and versatile catalyst in various chemical processes, creating new opportunities for developing more efficient and sustainable catalytic systems. There has been growing interest in the use of DILs in catalysis due to the factors mentioned above. For instance, Liu *et al.*[41] found that 1,1′-(hexane-1,6-diyl)-bis(3-methylimidazolium) dibromide produced 96% PC yield and 328 h^{-1} TOF at reaction conditions of 110 °C and 15 bar CO_2 pressure. Nevertheless, this single-component IL achieved sufficient catalytic activity in the presence of a co-catalyst (0.125 mmol ZnI_2). Shi *et al.*[20] prepared DILs catalysts such as $[IMCA]_2Cl_2$, $[IMCA]_2Br_2$, and $[IMCA]_2I_2$, which achieved 66.6, 74.4, 85.7% PC yields and high TOF of 41.6, 109.9, 233.2 h^{-1}, respectively. The catalysts performance follows the nucleophilicity order of the halide ions ($I^- > Br^- > Cl^-$). The application of these DILs catalysts to the conversion at low CO_2 concentration has not been investigated, and harsh reaction conditions were required (120 °C and 25 bar CO_2 pressure, and 4 h). As a result, problems with conventional monocationic ILs, such as their poor activity and stability, high catalyst amount, and difficult separation, have never been solved. Therefore, in order to overcome the above-mentioned problems, the design of dicationic ILs with multiple active sites was explored in this study. It is expected that the introduction of doubled halide anions and a dual positively charged cation will lead to a high-activity breakthrough that simultaneously activates multiple molecules; alkyl chain groups control the stability of DILs, allowing for a simplified separation process. To the best of our knowledge, DPzILs have not been observed to catalyze the cycloaddition of propylene oxide (PO) and CO_2 to propylene carbonate (PC).

In this study, eight novel dicationic pyrazolium ionic liquids were first synthesized. Then, their catalytic activity for the cycloaddition of CO_2 and PO was investigated under mild reaction conditions without any co-catalyst, metal, or solvent. The influence of alkyl chain lengths in the dication and different halide anions on catalytic performance is studied. The optimal reaction conditions, including reaction temperature, CO_2 pressure, catalyst amount, and reaction time, were investigated. The reusability of the catalyst and its broad applicability to different epoxides were also considered. Furthermore, the reaction mechanism was thoroughly investigated using FT-IR and ^1H NMR techniques in conjunction with density functional theory (DFT) study. Dicationic pyrazolium ILs may establish a distinct category of highly efficient CO_2 fixation catalysts.

2. Experimental section

2.1. Materials and instruments

The reagents and chemicals used in this study were of analytical grade and were obtained from Aladdin Chemical Company with a purity of >99%. Additional purification was not performed. CO_2 gas with a purity of 99.95% was supplied by Beijing Analytical Instrument Factory. The ^1H and ^{13}C NMR spectra of DPzILs were examined using a Bruker AVANCE III 600 MHz spectrometer, with DMSO as the deuterated solvent and tetramethylsilane (TMS) as the internal standard. The molecular weights of the DPzILs were measured *via* electrospray ionization-mass spectrometry (ESI-MS) using impact HD (Bruker, Germany) in acetonitrile solvent. Fourier transform infrared (FTIR) spectroscopy (Thermo Nicolet 380) was used to examine the chemical composition of the samples using anhydrous KBr as the reference material. On a Vario EL Cube elemental analyzer, elemental analysis (C/H/N) was performed. Using an empty crucible as the reference, TG-DTA measurements to determine the decomposition temperature of the samples were performed on a DTG-60H thermal analyzer (Shimadzu, Japan) at a heating rate of 10 °C min^{-1}. Gas chromatography (GC) analyzes were performed on GC-7890A (Agilent Technologies) using a flame ionization detector. GC-MS (GCMS-QP2020) was used to determine the composition of the products.

2.2. General procedure for the synthesis of dicationic pyrazolium ionic liquids

Eight new dicationic pyrazolium ionic liquids were synthesized with slight adjustments to the original literature.[37] The synthetic process used to produce the

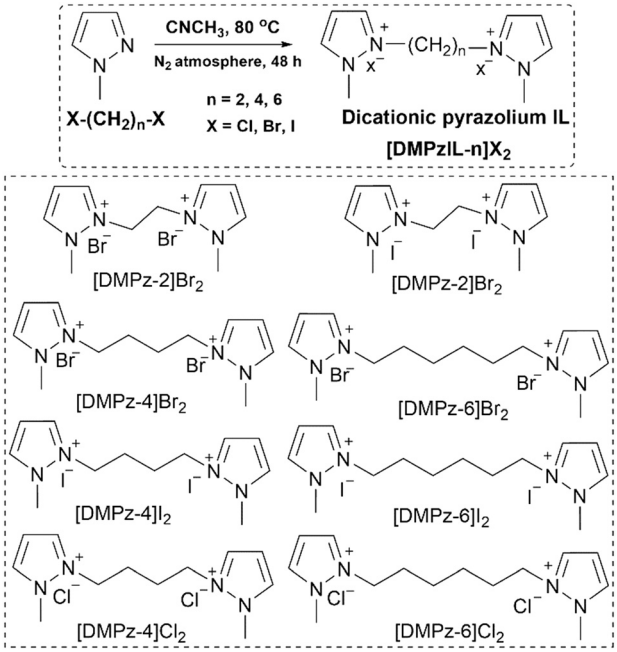

Scheme 2 Synthetic route and structures of dicationic pyrazolium ILs.

DPzILs is illustrated in Scheme 2. For example, 2,2′-(hexane-1,6-diyl)-bis(1-methylpyrazolium) diiodide ([DMPz-6]I_2) was synthesized by the following method: In a three-necked bottle, 1-methyl pyrazole (4.105 g, 0.05 mol) and 1,6-diiodohexane (16.899 g, 0.05 mol) were dissolved in 18 mL acetonitrile, and the mixture was agitated at room temperature for one hour. The mixture was then stirred under N_2 protection at 80 °C for 48 h. When the reaction was completed, the remaining solvent was evaporated using a rotary evaporator, and the resulting residue was subsequently washed with ethyl acetate (10 mL × 3) to remove impurities through centrifugation. Finally, the obtained DPzIL was dried for 24 h at 60 °C in a vacuum oven to produce the pure pale yellow solid ([DMPz-6]I_2). ^{1}H NMR (600 MHz, DMSO-d_6) δ (ppm) 8.60–8.48 (m, 2H, Pz–H), 6.89 (t, J = 3.2 Hz, 2H, Pz–H), 4.49 (t, J = 7.4 Hz, 2H, Pz–H), 4.16 (d, J = 7.7 Hz, 6H, –CH_3), 3.28 (t, J = 6.9 Hz, 4H, –CH_2–), 1.81 (dt, J = 48.2, 7.5 Hz, 4H, –CH_2–), 1.46–1.27 (m, 4H, –CH_2–). ^{13}C NMR (151 MHz, DMSO-d_6): δ (ppm) 139.46–136.51 (m), 107.64 (d, J = 4.4 Hz), 48.96 (d, J = 47.2 Hz), 37.61, 29.76 (d, J = 80.3 Hz), 25.24, 7.63. MS (ESI): m/z 124.0995 $[C_7H_{12}N_2]^{2+}$; 126.8985 $[I^-]$. Other DPzILs were prepared using the same method. Fig. S1–S27† show the spectra of eight dicationic pyrazolium ILs that were tested with ^{1}H/^{13}C NMR and ESI-MS.

2,2′-(Butane-1,4-diyl)-bis(1-methylpyrazolium)diiodide ([DMPz-4]I_2), pale yellow solid. ^{1}H NMR (600 MHz, DMSO-d_6): δ (ppm) 8.61–8.50 (m, 2H, Pz–H), 6.90 (p, 2H, Pz–H), 4.62–4.49 (m, 2H, Pz–H), 4.18 (d, 6H, –CH_3), 3.32 (t, J = 6.9 Hz, 4H, –CH_2–), 1.97–1.74 (m, 4H, –CH_2–). ^{13}C NMR (151 MHz, DMSO-d_6): δ (ppm) 138.64, 107.60, 49.08, 37.38 (d, J = 21.9 Hz), 29.07, 25.97. ^{13}C NMR (151 MHz, DMSO-d_6): δ (ppm) 138.87, 130.85, 105.55, 45.11, 38.76, 29.91. MS (ESI): m/z 219.029 $[C_{12}H_{20}N_4]^+$; 126.8963 $[I^-]$.

2,2′-(Ethane-1,2-diyl)-bis(1-methylpyrazolium)diiodide ([DMPz-2]I_2), black liquid. ^{1}H NMR (600 MHz, DMSO-d_6): δ (ppm) 8.65–8.52 (m, 2H, Pz–H), 6.91 (t, J = 2.9 Hz, 2H, Pz–H), 4.60 (s, 2H, Pz–H), 4.22 (d, 6H, CH_3), 3.33 (d, J = 7.0 Hz, 4H, –CH_2–). ^{13}C NMR (151 MHz, DMSO-d_6): δ (ppm) 138.53 (d, J = 84.5 Hz), 107.15, 50.42, 41.86, 36.95.

2,2′-(Hexane-1,6-diyl)-bis(1-methylpyrazolium)dibromide ([DMPz-6]Br_2), white solid. ^{1}H NMR (600 MHz, DMSO-d_6): δ (ppm) 8.56 (d, J = 22.5 Hz, 2H, Pz–H), 6.88 (s, 2H, Pz–H), 4.48 (s, 2H, Pz–H), 4.17 (d, 6H, –CH_3), 3.40 (s, 4H, –CH_2-), 1.82 (d, J = 22.1 Hz, 4H, –CH_2–), 1.37 (d, J = 46.1 Hz, 4H, –CH_2–). ^{13}C NMR (151 MHz, DMSO-d_6): δ (ppm) 137.90 (d, J = 176.5 Hz), 107.54 (d, J = 2.9 Hz), 49.72 (d, J = 4.9 Hz), 37.39, 30.07–27.42 (m), 25.09 (d, J = 66.5 Hz), 9.32. MS (ESI): m/z 124.0995 $[C_7H_{12}N_2]^{2+}$; 80.908 $[Br^-]$.

2,2′-(Butane-1,4-diyl)-bis(1-methylpyrazolium)dibromide ([DMPz-4]Br_2), white solid. ^{1}H NMR (600 MHz, DMSO-d_6): δ (ppm) 8.73–8.51 (m, 2H, Pz–H), 6.90 (q, J = 3.0 Hz, 2H, Pz–H), 4.61 (p, J = 34.3, 6.7 Hz, 2H, Pz–H), 4.21 (d, J = 17.3 Hz, 6H, –CH_3), 3.60 (t, J = 6.7 Hz, 4H, –CH_2–), 2.05–1.79 (m, 4H, –CH_2 –). ^{13}C NMR (151 MHz, DMSO-d_6): δ (ppm) 138.87, 130.85, 105.55, 45.11, 38.76, 29.91. MS (ESI): m/z 219.0266 $[C_{12}H_{20}N_4]^+$; 80.909 $[Br^-]$.

2,2′-(Ethane-1,2-diyl)-bis(1-methylpyrazolium)dibromide ([DMPz-2]Br_2), brown solid. ^{1}H NMR (600 MHz, DMSO-d_6): δ (ppm) 8.63 (t, J = 3.7 Hz, 2H, Pz–H), 6.93 (t, J = 2.9 Hz, 2H, Pz–H), 4.94 (t, J = 5.6 Hz, 2H, Pz–H), 4.18 (d, J = 29.3 Hz, 6H, –CH_3), 1.47 (t, J = 7.2 Hz, 4H, –CH_2–). ^{13}C NMR (151 MHz, DMSO-d_6): δ (ppm) 139.05 (d, J = 84.5 Hz), 107.68, 50.94, 42.38, 37.48. MS (ESI): m/z 190.992 $[C_{10}H_{16}N_4]^+$; 80.9083 $[Br^-]$.

2,2′-(Hexane-1,6-diyl)-bis(1-methylpyrazolium)dichloride ([DMPz-6]Cl_2), colorless liquid. ^{1}H NMR (600 MHz, DMSO-d_6): δ (ppm) 7.66 (d, J = 2.1 Hz, 2H, Pz–H), 7.39 (d, J = 1.8 Hz, 2H, Pz–H), 6.20 (t, J = 2.0 Hz, 2H, Pz–H), 3.83 (d, 6H, –CH_3), 3.63 (t, J = 6.6 Hz, 4H, –CH_2–), 1.72 (t, J = 6.8 Hz, 4H, –CH_2–), 1.44–1.36 (m, 4H, –CH_2–). ^{13}C NMR (151 MHz, DMSO-d_6): δ (ppm) 138.86, 130.82, 105.53, 45.71, 38.75, 32.35, 25.98. MS (ESI): m/z 124.0935 $[C_7H_{12}N_2]^{2+}$.

2,2′-(Butane-1,4-diyl)-bis(1-methylpyrazolium)dichloride ([DMPz-4]Cl_2), colorless liquid. ^{1}H NMR (600 MHz, DMSO-d_6): δ (ppm) 7.66 (d, J = 2.1 Hz, 2H, Pz–H), 7.39 (d, J = 1.8 Hz, 2H, Pz–H), 6.21 (t, J = 2.0 Hz, 2H, Pz–H), 3.83 (d, 6H, –CH_3), 3.68 (m, J = 6.3, 3.6, 2.1 Hz, 4H, –CH_2–), 1.85 (h, J = 3.0 Hz, 4H, –CH_2–). ^{13}C NMR (151 MHz, DMSO-d_6): δ (ppm) 138.87, 130.85, 105.55, 45.11, 38.76, 29.91. MS (ESI): m/z 124.0935 $[C_7H_{12}N_2]^{2+}$.

2.3. Cycloaddition of CO_2 with PO

Epoxides and DPzILs were first added to a stainless steel high-pressure microreactor (25 mL) equipped with a magnetic stirrer at ambient temperature. CO_2 was then added to the reaction vessel at a pressure of 1 to 25 bar and the temperature was adjusted to the desired level. The chemical reaction proceeded at temperatures between 40 and 120 °C for a duration of 1 to 15 h. After the reaction, the reactor was

cooled to room temperature and the excess CO_2 pressure was carefully released. The products were extracted from the homogenized solution by centrifugation and analyzed by GC.

3. Results and discussion

3.1. Characterization of dicationic pyrazolium ILs

The DPzILs underwent analytical analysis, including $^1H/^{13}C$ NMR, ESI-MS, EA, and FT-IR, to verify the successful synthesis of the intended structures (Scheme 2). In the $^1H/^{13}C$ NMR spectra analysis, the structures exhibited a high degree of correspondence with the characteristic peaks. For instance, in the case of [DMPz-6]I_2, seven distinct peaks were observed, with the number of hydrogens directly proportional to the integrated areas (Fig. 1). In addition, the $^1H/^{13}C$ NMR spectra of eight DPzILs are presented in Fig. S1–S16.† The ESI-MS data revealed the molecular weights of the DPzILs. For [DMPz-6]I_2, the positively charged ion $[C_7H_{12}N_2]^{2+}$ (*m*/*z* 124.0995) peak and the negatively charged ion $[I^-]$ (*m*/*z* 126.899) peak are shown in Fig. 2. The ESI-MS findings demonstrated that every DPzIL was successfully and impurity-freely produced. The spectra depicting the particulars of the other seven DPzILs are shown in Fig. S17–S27.†

According to the FT-IR investigation, the study illustrated in Fig. 3 displays the appearance of a peak within the 2800–3100 cm^{-1} range, which signifies the existence of CH_3 groups in the pyrazolium ring and the alkyl chains of the DPzILs (aromatic C–H stretching bands). The peaks observed at 1600–1680 cm^{-1} indicate the stretching vibrations associated with a carbon–carbon double bond (C=CH stretch) present in the pyrazolium ring of the catalysts. Identifying detectable peaks within the frequency range of 1500–1540 cm^{-1} indicates the C=N stretching vibration associated with the pyrazole ring of DPzILs. Furthermore, elemental analysis was conducted. The C/N molar ratios for [DMPz-6]I_2, [DMPz-6]Br_2, [DMPz-4]I_2, [DMPz-4]Br_2, [DMPz-2]I_2, and [DMPz-2]Br_2 were determined and are presented in Table S1.† The measured values were in good agreement with the theoretical molecular weights of the compounds. Specifically, the C/N molar ratios were 3.41, 3.60, 3.12, 3.02, 2.49, and 2.48, respectively. Overall, the successful synthesis of dicationic pyrazolium ionic liquids was confirmed by the above mentioned analytical techniques.

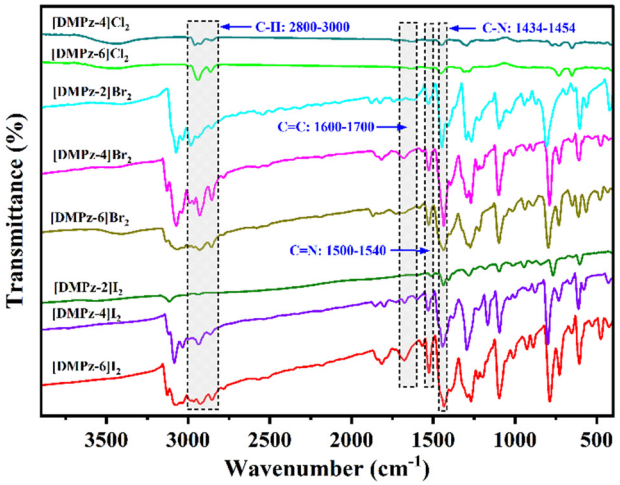

Fig. 2 FT-IR spectra of the DPzILs.

3.2. Catalysts screening for CO_2 cycloaddition reaction

Table 1 shows the results of a systematic evaluation of high-activity DPzILs with different alkyl chain lengths and a range of halide ions (Cl^-, Br^-, or I^-) in a rational screening process. A blank sample was used to test the catalyst addition. Entry 1 shows that PO conversion did not occur in the absence of the catalyst.

To better understand how structural modifications affect the catalytic performance of the synthesized DPzILs, catalysts

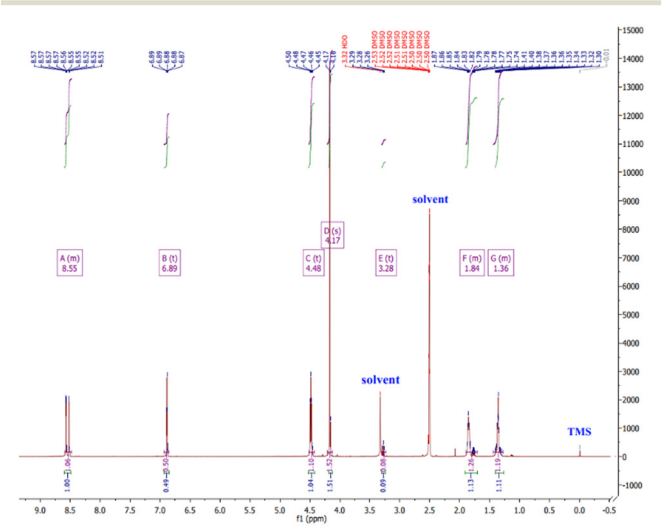

Fig. 1 ^1H NMR spectrum of [DMPz-6]I_2.

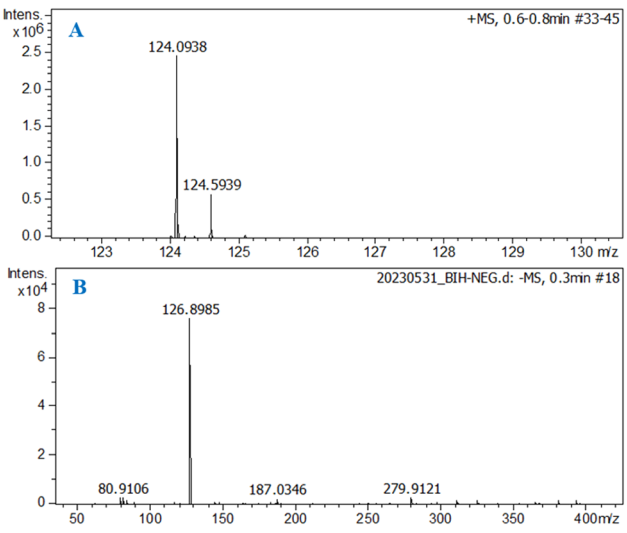

Fig. 3 ESI-MS spectra of [DMPz-6]I_2. Positive $[C_7H_{12}N_2]^{2+}$ (A) and negative mode $[I^-]$ (B).

Table 1 Screening of catalysts for the cycloaddition of CO_2 and PO[a]

Entry	Catalyst	Yield[e] (%)	Selectivity[e] (%)	TOF[f] (h^{-1})
1	Blank	None	None	None
2	[DMPz-2]I_2	79.4	100	42.5
3	[DMPz-4]I_2	93.8	100	50.2
4	[DMPz-6]I_2	97.9	99.9	52.4
5	[DMPz-6]Cl_2	45.8	99.8	24.5
6	[DMPz-6]Br_2	97.0	100	51.9
7	[DMPz-4]Br_2	95.0	100	50.8
8	[DMPz-2]Br_2	80.8	99.9	43.3
9	[DMPz-4]Cl_2	18.9	99.4	10.1
10[b]	[DMPz-6]I_2	83.2	100	111.4
11[b]	[DMPz-6]Br_2	72.2	99.9	39.4
12[b]	[DMPz-6]Cl_2	29.5	99.7	96.7
13[c]	[DMPz-6]I_2	95.9	100	76.2
14[c]	[DMPz-6]Br_2	95.7	100	77.1
15[c]	[DMPz-6]Cl_2	29.2	99.7	23.4
16[c]	[DMPz-4]I_2	90.6	99.9	18.2
17[c]	[DMPz-4]Br_2	87.6	99.9	70.4
18[c]	[DMPz-4]Cl_2	22.6	99.5	72.8
19[d]	[DMPz-6]I_2	98.3	100	197.3
20[d]	[DMPz-6]Br_2	96.8	99.9	188.0

[a] Reaction conditions: 20 mmol PO, catalyst 2.9 mol%, initial CO_2 pressure 10 bar, temperature 80 °C, time 15 h. [b] Reaction conditions: 20 mmol PO, catalyst 2.9 mol%, initial CO_2 pressure 5 bar, temperature 70 °C, and reaction time 6 h. [c] Reaction conditions: 20 mmol PO, catalyst 2.9 mol%, initial CO_2 pressure 5 bar, temperature 70 °C, and reaction time 10 h. [d] Reaction conditions: 30 mmol PO, catalyst 3.8 mol%, initial CO_2 pressure 10 bar, temperature 90 °C, time 8 h. [e] Yield and selectivity were determined by GC. [f] Moles of PC produced per mole of DPzIL per hour.

with ethyl, butyl, and hexyl linkers were tested. It is important to note that alkyl chain lengths have a significant effect on catalytic activity and PC production.[42] The study found a correlation between the number of alkyl chain groups and the PC yield of DPzILs. Specifically, the product yields increased with an increase in alkyl chain lengths (entries 2–4). [DMPz-6]I_2 with hexyl chain length exhibited the highest PC yield of 97.9% and 100% selectivity (entry 4), followed by [DMPz-4]I_2 reaching 93.8% PC yield (entry 3), and [DMPz-2]I_2 obtained 79.4% yield (entry 2). Similarly, [DMPz-6]Br_2 (entry 6) demonstrated a higher activity (97.0% yield) compared with [DMPz-4]Br_2 (entry 7, 95.0% yield) and [DMPz-2]Br_2 (entry 8, 80.8% yield).

In the case of [DMPz-6]I_2 and [DMPz-6]Br_2 applications, the hexyl linkers facilitated the access of PO and CO_2 to the dual-pyrazolium cationic catalytic sites, leading to enhanced substrate activation and higher reaction efficiency. The hexyl chain groups in [DMPz-6]I_2/[DMPz-6]Br_2 offer a more relaxed structure with fewer steric hindrances, enabling the reactants to approach the catalytic centers (N^+ sites of the dicationic pyrazolium ring) more easily. This enables the catalyst to create more efficient transition states and intermediates while catalyzing the reaction, resulting in increased activity. In addition, the hexyl chain groups are capable of influencing the electron density and distribution within the catalyst structure, thus leading to improved efficiency in electron transfer and conversion of CO_2 to propylene oxide. However, the ethyl linkers in compounds such as [DMPz-2]I_2 and [DMPz-2]Br_2 might experience greater steric hindrance and less flexibility, potentially restricting their catalytic effectiveness. Our findings match those of Guglielmero *et al.*,[43] who discovered that the catalysts from the DILs set containing hexyl chains exhibited superior catalytic activity compared with DILs with butyl substitutions.

The influence of various halide ions on catalyst activity was also explored. The polarized properties of the ILs and the electrical structure of the active centers of the catalysts are affected by the counteranions present in the ILs. According to our results, the order of catalytic activity of the halide ions is as follows: $I^- > Br^- > Cl^-$ (entries 4–6). The same trend was also found for entries 10–15. In general, the DPzILs containing Cl^- showed lower catalytic activity compared to DPzILs containing I^- or Br^- ions. For example, [DMPz-6]Cl_2 reached 45.8% PC yield and 24.5 h^{-1} TOF (entry 5), while [DMPz-6]I_2 and [DMPz-6]Br_2 (entries 4 and 6) achieved the PC yields of 97.9% and 97.0%, respectively. The same phenomenon was observed throughout the study. This is due to the larger size and lower electronegativity of diiodide, which might cause weakened interactions with the catalytic sites (N^+ centers of the dual-pyrazolium cation) and PO. This ultimately enhances substrate activation and reaction kinetics. In contrast, the smaller and more electronegative counteranions of dibromide and dichloride may interact more with the catalyst and reactants. This could lead to increased intermediate stability, greater steric hindrance, and hindered reactant transport, potentially limiting catalytic activity.[44,45]

Consistent with earlier studies, the larger size and higher nucleophilicity of Br^- than Cl^- could lead to differences in their coordination sphere with the dicationic portion of the catalyst, resulting in enhanced PC production.[45] Moreover, bromide can donate its lone pair of electrons to establish a bond with another reactant. This augmented nucleophilicity adds to its increased catalytic activity. Our study found that bromide or iodide ions did not significantly impact the catalysts' performance, as there were no major differences in their results. Of all DPzILs tested, [DMPz-4]Cl_2 exhibited the least effective catalytic performance, producing only 18.9% yield with 99.4% selectivity (entry 9). Moreover, [DMPz-6]I_2 displayed an impressive TOF of 111.4 h^{-1} (entry 10) and achieved a remarkable product yield of 95.9% and 100% selectivity under mild reaction conditions (70 °C and 5 bar CO_2 pressure) (entry 10). In addition, increasing the reaction temperature to 90 °C and CO_2 pressure to 10 bar (entries 19 and 20) with increased catalyst amount (3.8 mol%) results in slightly higher yields (98.3% and 96.8%, respectively) for [DMPz-6]I_2 and[DMPz-6]Br_2 catalysts, confirming the importance of sufficient catalyst concentration in the reaction system.[46] Furthermore, the selectivity remains >99% for all DPzILs catalytic activity experiments. When conducting thermogravimetric analysis to examine the thermal stability of five chosen DPzILs and determine their decomposition temperatures, it was revealed that [DMPz-6]I_2 remains intact

even at a high temperature of 183 °C (Fig. S28†). In general, the cycloaddition reaction substantially benefited from [DMPz-6]I_2, a catalyst comprising a hexyl chain length and a diiodide ion. This catalyst demonstrated exceptional efficiency.

3.3. Effects of reaction conditions

The primary reaction parameters for the conversion of PO were thoroughly investigated sequentially, including the reaction temperature, initial CO_2 pressure, catalyst loading, and reaction time. The catalytic activity of [DMPz-6]I_2 was examined as a case study. Experiments were conducted to reveal the effect of the reaction temperature, and the results are presented in Fig. 4. The figure indicates an increasing trend in PC yield and selectivity. Increasing the reaction temperature from 80 °C to 100 °C resulted in a 17.0% increase in PC yield. The data indicate a gradual increase in product yield within the temperature ranges of 40–50 °C and 80–100 °C, with values rising from 15.7% to 20.2% and 80.7% to 97.4%, respectively. The product yield increases significantly from 20.3% to 80.7% within the 50–80 °C range. Then, with further increase in temperature, the PC yield experienced a marginal decrease from 97.4% to 94.9% within the temperature interval of 100–120 °C, which can be attributed to the development of side reactions.[34] In terms of selectivity, the [DMPz-6]I_2 catalyst showed remarkable stability, maintaining a level above 99% throughout the process.

Subsequently, the initial CO_2 pressure significantly affects the catalytic activity (Fig. 5). The PC yield increased by 46.8% when the CO_2 pressure was varied from 1 to 5 bar. At a CO_2 pressure of 10 bar, the PC yield obtained was 89.7%; thus, 10 bar was the optimal initial CO_2 pressure. However, a marginal decrease in PC yield was observed upon attaining a CO_2 pressure of 10 bar. Initially, the elevation in CO_2 pressure would increase the concentration of the reactant,

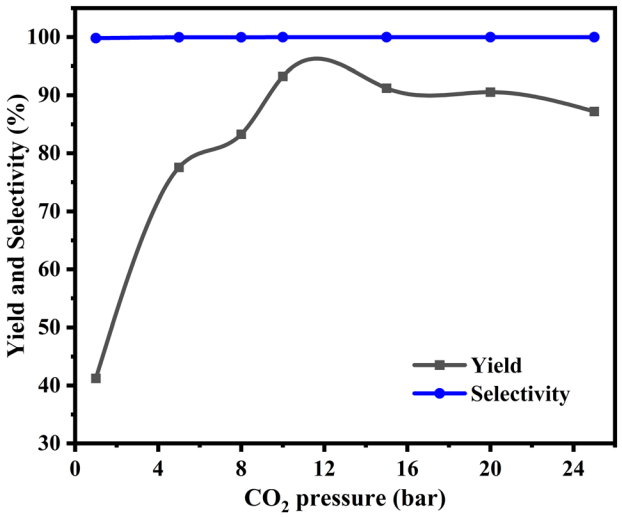

Fig. 5 Influence of CO_2 pressure on product yield and selectivity: PO 20 mmol, [DMPz-6]I_2 300 mg, temperature 80 °C, and time 6 h.

which would be beneficial for promoting the catalytic reaction. The introduction of additional CO_2 into the system would reduce the concentration of ILs, which would suppress the reaction to some extent, ultimately leading to a decrease in product yield. Throughout the process, the selectivity of the PC remained impervious, exceeding 99%.

The effect of catalyst loading on PC yield and selectivity was also investigated. As shown in Fig. 6, the yield of PC increased dramatically from 7.3% to 72.2% as the catalyst amount increased from 30 to 200 mg. Increasing the amount of [DMPz-6]I_2 from 200 to 300 mg resulted in a slight increase in the PC yield, which reached 93.3% and 99.9% selectivity. The experimental results show that the product yield remained almost constant (93.3–94.8%) despite the increase in catalyst amount from 300 to 500 mg. Similarly,

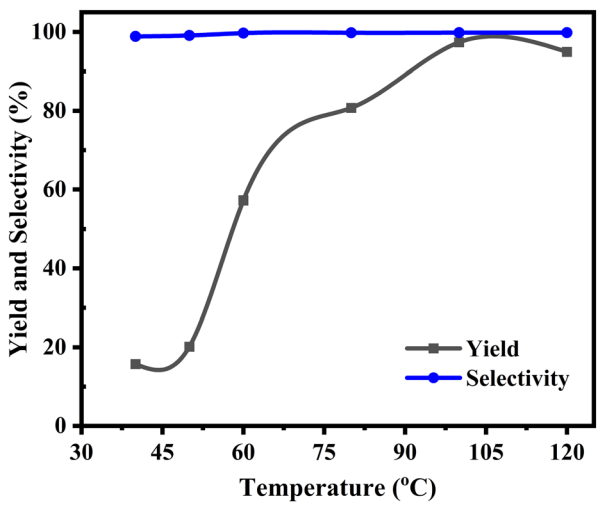

Fig. 4 Influence of temperature on product yield and selectivity: PO 20 mmol, [DMPz-6]I_2 300 mg, initial CO_2 pressure 10 bar, and time 6 h.

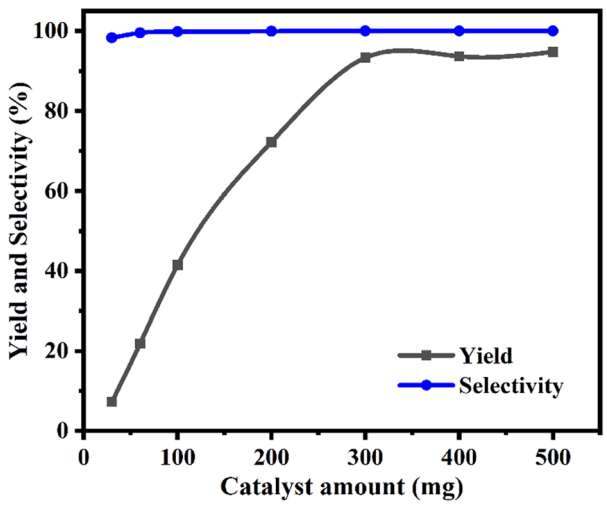

Fig. 6 Effect of catalyst dosage on product yield and selectivity. PO 20 mmol, temperature 80 °C, initial CO_2 pressure 10 bar, and time 6 h.

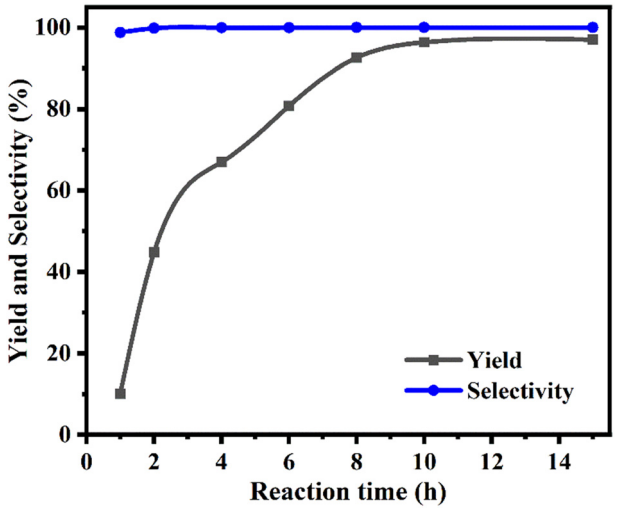

Fig. 7 Effect of reaction time on product yield and selectivity. PO 20 mmol, [DMPz-6]I_2 300 mg, temperature 80 °C, and initial CO_2 pressure 10 bar.

PC exhibited a selectivity greater than 99% in all experiments. The optimum amount of catalyst for the reaction was 300 mg (2.9 mol%).

Fig. 7 depicts the correlation between reaction time and PC production and selectivity. During the initial 10-hour period, there was a significant increase in the yield of PC from 10.1% to 96.4%. The extension of the reaction time may facilitate the sequestration of carbon dioxide to a limited extent. The process exhibited a consistent selectivity of over 98.8% throughout, with no discernible impact from reaction time. Thus, a reaction time of 10 h was the optimal choice. In summary, the most favourable reaction parameters were determined to be a temperature of 100 °C, CO_2 pressure of 10 bar, catalyst amount of 300 mg, and reaction time of 10 h.

3.4. Comparison of the DPzILs catalytic performance with previous literature

To evaluate the advantages of the catalytic efficiency of the as-prepared DPzILs, the research concluded with a comparison of the performance of the present catalysts with that of the previously reported monocationic pyrazolium ILs and dicationic imidazolium ILs (Table 2). Significantly, the alkyl pyrazolium ILs and protic pyrazolium ILs (entries 1 and 2) had a reaction temperature of 130 °C, exceeding the temperature of the present study by a range of 30–60 °C. The hydroxyl- and amino-functionalized pyrazolium ILs (entries 3 and 4) reacted at 110 °C, a difference of 10 °C from the temperature used in this study. For the amino-functionalized pyrazolium ILs (entry 5), the CO_2 pressure remained elevated at 15 bar despite lowering the reaction temperature to 110 °C. When DPzILs were compared to the reported DILs catalysts, entries 14–16 of the current work show strong performance with yields ranging from 83.2% to 97.9% under mild conditions. These results highlight the important role of multiple active sites such as hydrogen bond donors (C3/C5–H), Lewis basic tertiary amines (N^+ sites), and halide anions in the structure of DPzILs catalysts, suggesting their potential utility in practical applications. In particular, the competitive yields and TOF values in entries 13–16 suggest that [DMPz-6]I_2 and [DMPz-6]Br_2 are promising homogeneous catalysts for the CO_2 cycloaddition, comparable to or even better than several previously reported single-component ILs.

3.5. Catalytic performance of dicationic pyrazolium ionic liquid in diluted CO_2

Large-scale manufacturing depends on the carbon dioxide source for the epoxide cycloaddition reaction. From flue gases, CO_2 capture, usage, and storage produce high-value compounds. Cycloaddition of low-concentration CO_2 from

Table 2 Comparison of reported single-component pyrazolium ILs and dicationic imidazolium ILs with the current work

Entry	Catalyst	T (°C)/t (h)/CO_2 (bar)	Yield (%)	TOF (h^{-1})	Ref.
1[a]	DEPzI	120/4/20	96.1	—	32
2[a]	HEPzI	130/4/20	90.21	22.55	43
3[a]	HEEMPzBr	110/4/10	92.9	—	35
4[a]	[EPzPNH$_3$]Br_2	70/24/5	96.1	—	37
5[a]	APEPzBr	110/4/15	94	23.57	36
6[b]	ImIL/ZnI_2 (1 : 2 ratio)	110/2/15	96	328	41
7[b]	[$CH_2CHOHCH_2$(Mim)$_2$]Br_2	70/16/4	95	2.0	47
8[b]	[$CH_2CH_2CH_2$(Mim)$_2$]Br_2	70/16/4	58	1.2	47
9[b]	C_6(MIM)$_2$ 2Br	80/20/10	47	—	43
10[b]	[IMCA]$_2Cl_2$	120/4/25	66.6	41.6	20
11[b]	[IMCA]$_2Br_2$	120/4/25	74.4	109.9	20
12[b]	[IMCA]$_2I_2$	120/4/25	85.7	233.2	20
13[c]	[DMPz-6]I_2	100/10/10	97.9	52.4	This work
14[c]	[DMPz-6]I_2	70/6/5	83.2	111.4	This work
15[c]	[DMPz-6]I_2	70/10/5	97.9	76.2	This work
16[c]	[DMPz-6]Br_2	70/10/5	95.7	77.1	This work

[a] Monocationic pyrazolium IL. [b] Dicationic imidazolium ionic liquid. [c] Dicationic pyrazolium ionic liquid.

flue gas and epoxides requires strong catalysts with high catalytic activity. Industrially harvested CO_2 contains impurities such as CO, H_2S, NOx, SOx, and water. Their effects on the catalytic system are crucial because they can inhibit active sites or degrade the catalyst. Limited research has been conducted on the impact of using CO_2 with reduced purity levels, which may comprise pollutants usually in flue gases.[18,48]

To assess the catalytic efficiency of [DMPz-6]I_2 at low CO_2 concentrations, five experiments were performed to replicate the cycloaddition reaction between diluted CO_2 and PO. The concentration of CO_2 was manipulated by altering its mole ratio to N_2 (*i.e.*, 10% CO_2 + 90% N_2, 20% CO_2 + 80% N_2, 40% CO_2 + 60% N_2, 60% CO_2 + 40% N_2, and 80% CO_2 + 20% N_2). Based on the results of the experiments shown in Fig. 8, when [DMPz-6]I_2 is exposed to 80% CO_2, it has a PC yield of 94.1%. This value is 3.9% lower than the PC yield obtained when employing pure CO_2 as the gas source.[49] A decrease in PC yield is observed when the concentrations of CO_2 are 60%, 40%, and 20%, resulting in yields of 94.1%, 63.2%, and 36.0%, respectively. The yield of PC is shown to be only 6.8% when the concentration of CO_2 reaches 10%. The observed drop can be attributed to an incomplete reaction resulting from inadequate CO_2. Furthermore, it is observed that the concentration of CO_2 exhibits minimal influence on the selectivity of PC (98–100%). In brief, the catalytic activity of the [DMPz-6]I_2 catalyst is sufficient for facilitating the cycloaddition process between epoxide and CO_2 at low concentrations.

3.6. Catalyst recycling studies

The performance evaluation of ionic liquid catalysts, especially homogeneous catalysts, includes a significant consideration of recyclability as an important criterion. Using [DMPz-6]I_2 as the model catalyst, the coupling reaction of CO_2 and PO was performed under the best possible conditions. The results are shown in Fig. 9. The [DMPz-6]I_2 catalyst exhibited good recyclability for the cycloaddition reaction of CO_2 with PO, as evidenced by its ability to be reused up to seven times with only a slight change in PC yield (1.0–3.6%). Later, the catalyst reused five times was subjected to TGA and FT-IR tests, which showed that the decomposition temperature remained unchanged (Fig. 10), and the FT-IR spectrum did not show any changes in the chemical composition of the sample (Fig. S29†). Importantly, the [DMPz-6]I_2 catalyst demonstrated the ability to undergo seven recycling runs without experiencing any degradation.

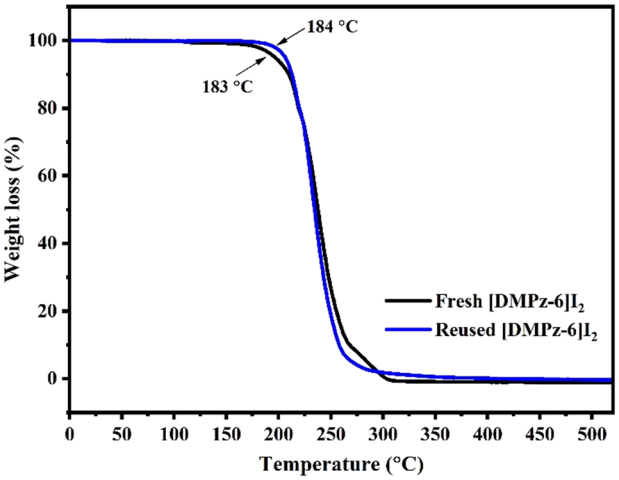

Fig. 9 TGA curves of fresh and reused [DMPz-6]I_2.

3.7. Catalytic activity of substrates scopes of epoxides

In order to assess the overall versatility of [DMPz-6]I_2 in the chemical fixation of CO_2, various terminal epoxides were subjected to experiments, and the findings are summarized in Table 3. The substrates examined in this study include PO,

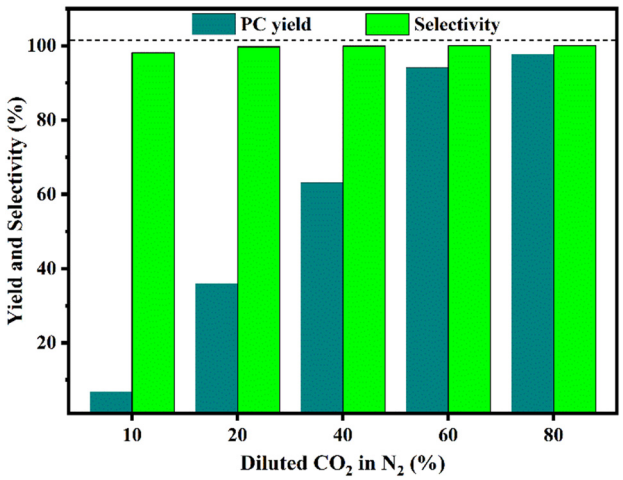

Fig. 8 Catalytic performance of [DMPz-6]I_2 on diluted CO_2. PO 20 mmol, catalyst 300 mg, 100 °C, and time 10 h.

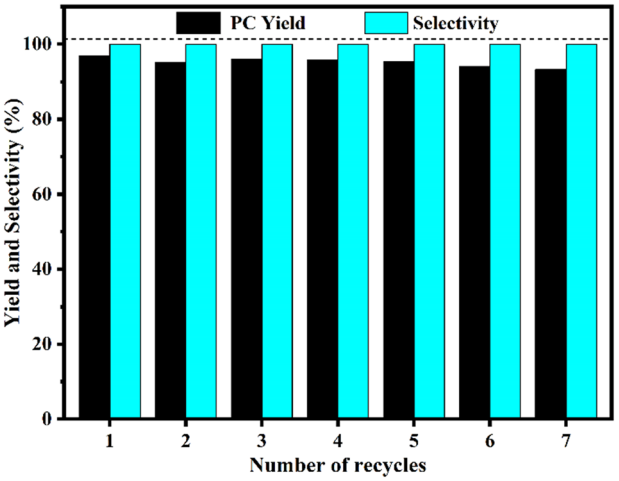

Fig. 10 Recyclability of [DMPz-6]I_2 on product yield and selectivity. PO 20 mmol, [DMPz-6]I_2 300 mg, CO_2 pressure 10 bar, time 10 h, and temperature of 100 °C.

Table 3 Cycloaddition of CO_2 and substrates catalyzed by [DMPz-6]I_2[a]

Entry	Epoxide	Cyclic carbonate	Yield[b] (%)	Sel.[b] (%)
1	 **1a**	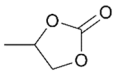 **1b**	97.7	99.9
2	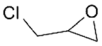 **2a**	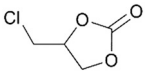 **2b**	96.7	98.5
3	 **3a**	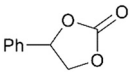 **3b**	93.7	99.9
4	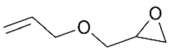 **4a**	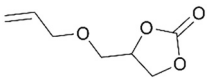 **4b**	93.6	99.9
5	 **5a**	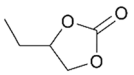 **5b**	66.2	99.9
6	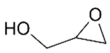 **6a**	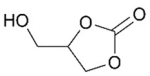 **6b**	79.3	99.9
7	 **7a**	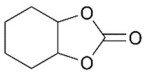 **7b**	37.9	99.7

[a] Reaction conditions: epoxide 30 mmol, [DMPz-6]I_2 300 mg, CO_2 pressure 10 bar, temperature 100 °C, and time 10 h. [b] PC yield and selectivity were determined by GC.

epichlorohydrin (ECH), styrene oxide (SO), allyl glycidyl ether (AGE), 1,2-butylene oxide (BO), glycidol, and the internal epoxide of cyclohexene oxide (CHO), which is generally considered to be a more difficult substrate for the cycloaddition reaction with CO_2 (entry 7). Overall, the study successfully converted seven epoxides to their respective cyclic carbonates with remarkable selectivity and high yields, as shown in entries 1–7. The yields of products **1b** and **2b** are comparable and significantly higher than those of the other entries. The results indicate that PO exhibited the highest PC yield of 97.7% and a selectivity of over 99% due to its lower steric hindrance.

Furthermore, ECH (**2a**) demonstrated a high product yield of 96.9% and can be considered an excellent reactive substrate. The remarkable performance of ECH (**2b**) can be elucidated by the electron-withdrawing impact of its substituent, which expedited the nucleophilic assault to initiate the opening of the epoxide ring.[42] The impact of the substituted group size on the C atom on product yield is insignificant, except for cyclohexene oxide. The observed trend indicates a decrease in response with an increase in the alkyl length of the epoxide, as evidenced by the comparison between entries 1 and 4–6. Using BO as a substrate resulted in a PC yield of 66.0% within 10 h (entry 4). This result can be attributed to BO's considerable steric hindrance and powerful electron-donating capability.

However, the catalytic activity declined with increasing steric hindrance from the side chain groups. The conversion rate of CHO (**7a**) was 37.9% over 10 h. The observed phenomenon can be rationalized on the basis of a steric barrier caused by the two rings of cyclohexene oxide, which impedes the nucleophilic attack of the iodide ion and consequently reduces the rate of ring opening. In particular, it can be concluded that the bulkiness of CHO is the main factor contributing to this effect. In conclusion, both steric and electronic factors are believed to be crucial in controlling the chemical coupling reaction between epoxides and CO_2. This study shows that nucleophilic attack facilitates the ring opening of PO. The [DMPz-6]I_2 catalyst has wide-ranging usefulness for a variety of epoxy substrates.

3.8. Study of the reaction mechanisms

Interaction between DPzILs and PO. The detailed reaction mechanisms were investigated using FT-IR and ^{1}H NMR characterizations, accompanied by DFT using the Gaussian 09 program package. To reduce computational expenses, the Br^- anion was substituted for the Cl^- and I^- anions in all DFT calculations. The geometries (Fig. S30†) for DPzILs-related structures were optimized using the B3LYP method in conjunction with the 6-311G++(d,p) basis set (B3LYP/6-311+

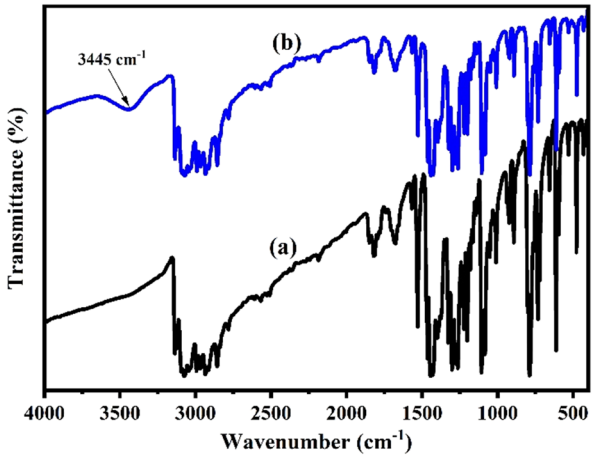

Fig. 11 FT-IR spectrum of [DMPz-6]I_2 with (a) and without PO (b).

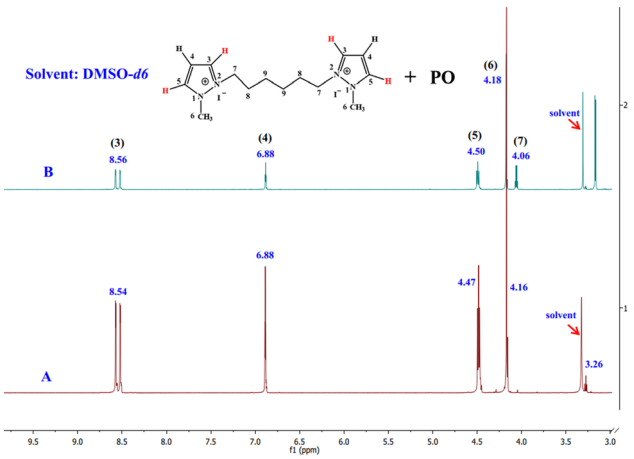

Fig. 12 ^{1}H NMR spectra of [DMPz-6]I_2 (A) without and (B) with PO.

+G(d,p)). The above study was performed to better understand the different catalytic activities of different DPzILs with altered alkyl chain lengths and halide anions. Initially, the ^{1}H NMR and FT-IR spectra of [DMPz-6]I_2 with and without PO were investigated to explore the hydrogen bonding interaction between the reactive hydrogen atom of the pyrazolium dication and PO.

The FT-IR spectra depicted in Fig. 11 reveal the appearance of a specific absorption at 3445 cm^{-1} in spectrum (b), which can be attributed to the stretching vibrations of the OH groups. This appearance indicates the formation of a C–O···H bond. The above result suggests that the hydrogen atoms in methylene-H can form a hydrogen bond with the oxygen atom of PO, thereby promoting the ring-opening of PO.[32]

Furthermore, the interaction between PO and DPzILs was confirmed by analyzing the ^{1}H NMR spectra (Fig. 12). The N–CH_3 and N–CH_2– proton signals in [DMPz-6]I_2, found at δ = 4.16 and 3.26 ppm, showed a shift to δ = 4.18 and 4.06 ppm, respectively. This signifies hydrogen bond formation between [DMPz-6]I_2 and PO. Similarly, a hydrogen atom located on the pyrazole rings at C3/C5 exhibited a chemical shift from

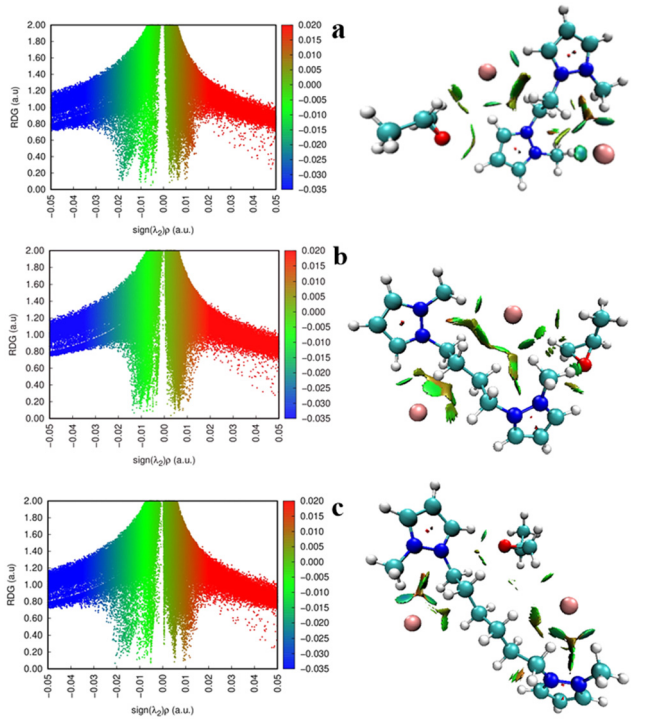

Fig. 13 NCI plots for (a) PO-[DMPz-2]Br_2, (b) PO-[DMPz-4]Br_2, and (c) PO-[DMPz-6]Br_2. The matching 3D graphs are shown on the right, with blue regions indicating strong electrostatic interactions and green regions indicating dispersive attractive interactions.

8.54/4.47 to 8.56/4.50 ppm. The formation of hydrogen bonds results in a downfield shift due to the deshielding effect it has on the hydrogen atom involved in the bond.[42] When hydrogen bonding occurs, the electron density around the hydrogen atom is reduced, resulting in deshielding from the external magnetic field, which is consistent with our findings. This reduced electron density increases the effective magnetic field strength experienced by the hydrogen nucleus.[50] As a result, its resonant frequency decreases, causing a downfield shift in the NMR spectrum.

Noncovalent interactions also significantly influence the improvement of catalytic performance. To provide additional evidence of the hydrogen bond interactions present in the cycloaddition, the DPzILs were subjected to noncovalent interaction (NCI) analysis using Multiwfn, and visual molecular dynamics (VMD),[34,42] as shown in Fig. 13. The DPzILs developed a strong hydrogen bond between the PO oxygen atom and the C3/C5 hydrogen of the pyrazole rings. Thus, the electrophilic attack was achieved by the combined influence of hydrogen bonding and electrostatic interaction throughout the ring-opening process.

Proposed reaction mechanism. The process of coupling CO_2 with PO typically involves a sequence of three stages, namely, the ring-opening of PO, CO_2 insertion, and ring-closure leading to the formation of PC, accompanied by catalyst regeneration. The emphasis is on the ring-opening of PO, which has been identified as the determinant of the overall reaction rate. It is well known that the ring-opening of

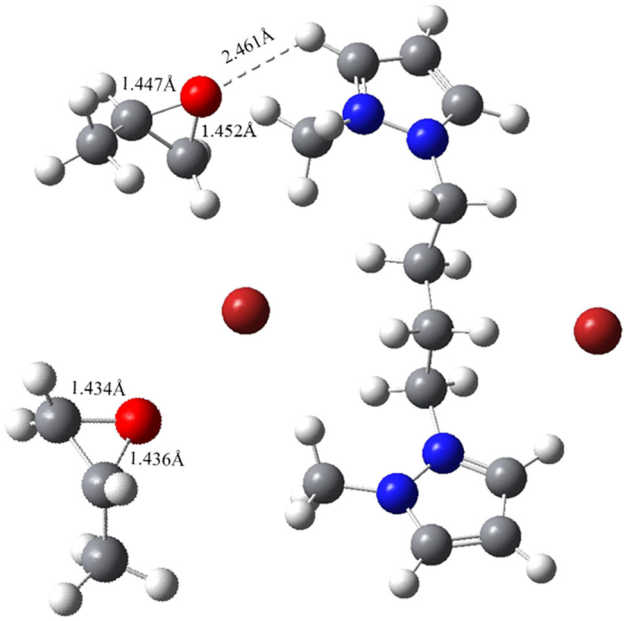

Fig. 14 Bond distances between DPzILs and PO from DFT study.

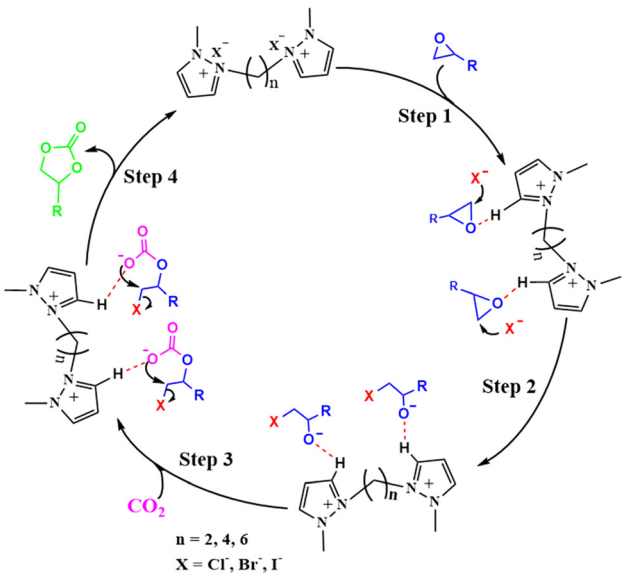

Scheme 3 The proposed reaction mechanism for the cycloaddition reaction.

PO is the synergistic result of both the electrophilic attack of the cation and the nucleophilic attack of the anion.[34] Therefore, the more active the hydrogen atom in the dication is, the stronger the electrophilic attack is. The DFT study revealed that the hydrogen bonding resulting from the pyrazole ring (C3/C5) primarily reduces the strength of the C–O bond interaction. Initially, the C–O distances of PO were recorded as 1.434 Å. Upon mixing [DMPz-4]Br_2 and PO, the bond distances increased, with a value of 1.452 Å being verified (Fig. 14). The elongation of the bond length facilitates the ring-opening process of PO. The halide ion (X = $I^-/Br^-/Cl^-$) then attacked the carbon atom, leading to the cleavage of the epoxide ring. Multiple active sites allow anions to activate multiple epoxide molecules, thereby enhancing the efficiency of DPzILs. The presence of hydrogen bonds resulted in an increase in the bond lengths, thereby enhancing the probability of the reaction.

On the basis of the results of our study and the literature references.[20,42] we have proposed a plausible mechanism for the catalytic conversion of CO_2 to cyclic carbonate by DPzILs, as shown in Scheme 3. First, the oxygen atom of PO interacts with the C3/C5–H of the dual-positively charged pyrazolium rings. This interaction polarizes the C–O bond in the epoxide ring of PO, making the carbon atom more electrophilic (step 1). Next, to break the bond between PO and its ring, the halide ion (X^-) of DPzIL nucleophilically attacks the slightly hindered carbon atom (–CH_2–) of PO. This nucleophilic attack leads to the cleavage of the C–O bond in the epoxide ring, forming an intermediate oxyanion species (step 2). After that, the addition of carbon dioxide to the oxyanion species intermediate led to the formation of an alkyl carbonate intermediate (step 3). The final step involved the generation of PC through the intramolecular cyclization of the alkyl carbonate anion, while the release of the X^- anion facilitated the completion of the DPzIL catalyst regeneration process (step 4).

4. Conclusions

A series of novel dicationic pyrazolium ILs were successfully synthesized and used as catalysts for the cycloaddition reaction of CO_2. [DMPz-6]I_2, which possesses multiple interaction sites, displayed higher catalytic activity than other DPzILs, achieving an outstanding 95.9% PC yield and 100% selectivity under mild conditions (70 °C and 5 bar CO_2 pressure). [DMPz-6]I_2 exhibited excellent propylene carbonate production from diluted (waste) CO_2 with exceptional performance. In addition, [DMPz-6]I_2 exhibited consistent catalytic activity even after seven cycles of reuse. Furthermore, it showed a favorable efficiency in converting various terminal epoxides, resulting in satisfactory product yields. Finally, the reaction mechanism was consistently elucidated using ^{1}H NMR, FT-IR, and DFT calculations. This in-depth study revealed that the synergistic interaction of C3/C5–H from doubly charged pyrazolium rings (containing N^+ centers) linked by an alkyl chain group, combined with halide anions ($I^-/Br^-/Cl^-$), significantly improves the catalytic efficiency and cyclic carbonate yields. Dicationic pyrazolium ionic liquids demonstrate considerable promise as effective catalysts for carbon dioxide fixation in sustainable chemistry.

Author contributions

Jean Damascene Ndayambaje: conceptualization, methodology, validation, formal analysis, investigation, data curation, writing – original draft, writing review & editing, visualization. Irfan Shabbir: writing review & editing.

Qianmeng Zhao: writing review & editing. Li Dong: funding acquisition, project administration. Qian Su: conceptualization, methodology, writing review & editing. Weiguo Cheng: conceptualization, methodology, resources, funding acquisition.

Conflicts of interest

There are no conflicts to declare.

Acknowledgements

We gratefully acknowledge the support of the National Natural Science Foundation of China (No. 22078329, 21890763, 22178356) and the Key-Area Research and Development Program of Guangdong Province (No. 2020B0101370002).

References

1 Q.-W. Song, R. Ma, P. Liu, K. Zhang and L.-N. He, *Green Chem.*, 2023, **25**, 6538–6560.
2 T. Wang, D. Zheng, B. An, Y. Liu, T. Ren, H. Ågren, L. Wang, J. Zhang and M. S. G. Ahlquist, *Green Energy Environ.*, 2022, **7**, 1327–1339.
3 D. U. Nielsen, X.-M. Hu, K. Daasbjerg and T. Skrydstrup, *Nat. Catal.*, 2018, **1**, 244–254.
4 Y. Liu, S. Li, X. Yu, Y. Chen, X. Tang, T. Hu, L. Shi, M. Pudukudy, S. Shan and Y. Zhi, *Mol. Catal.*, 2023, **547**, 113344.
5 L. Deng, Q. Su, X. Tan, Y. Wang, L. Dong, H. He, Z. Li and W. Cheng, *Mol. Catal.*, 2022, **519**, 112153.
6 Q. Zhao, X. Yao, Q. Su, L. Deng, J. Chen, Y. Li, L. Dong, Z. Yang and W. Cheng, *ChemCatChem*, 2023, **15**, e202300754.
7 M. Zanatta, E. García-Verdugo and V. Sans, *ACS Sustainable Chem. Eng.*, 2023, **11**, 9613–9619.
8 S. Chen, R. An, Y. Li, Y. Zhu, X. Zhu, R. Liu and X. Li, *Catal. Sci. Technol.*, 2021, **11**, 6498–6506.
9 C. A. Obasanjo, G. Gao, J. Crane, V. Golovanova, F. P. García de Arquer and C.-T. Dinh, *Nat. Commun.*, 2023, **14**, 3176.
10 H. Gou, X. Ma, Q. Su, L. Liu, T. Ying, W. Qian, L. Dong and W. Cheng, *Phys. Chem. Chem. Phys.*, 2021, **23**, 2005–2014.
11 Y. Zou, Y. Ge, Q. Zhang, W. Liu, X. Li, G. Cheng and H. Ke, *Catal. Sci. Technol.*, 2022, **12**, 273–281.
12 L. Guo, K. J. Lamb and M. North, *Green Chem.*, 2021, **23**, 77–118.
13 W. Qian, X. Ma, L. Liu, L. Deng, Q. Su, R. Bai, Z. Zhang, H. Gou, L. Dong, W. Cheng and F. Xu, *Green Chem.*, 2020, **22**, 5357–5368.
14 C. Ma, F. Xu, W. Cheng, X. Tan, Q. Su and S. Zhang, *ACS Sustainable Chem. Eng.*, 2018, **6**, 2684–2693.
15 X. Ma, J. Yu, Y. Hu, J. Texter and F. Yan, *Ind. Chem. Mater.*, 2023, **1**, 39–59.
16 H. Tong, Y. Qu, Z. Li, J. He, X. Zou, Y. Zhou, T. Duan, B. Liu, J. Sun and K. Guo, *Chem. Eng. J.*, 2022, **444**, 135478.
17 W. Zhang, Y. Mei, P. Wu, H.-H. Wu and M.-Y. He, *Catal. Sci. Technol.*, 2019, **9**, 1030–1038.
18 Y. Tong, R. Cheng, H. Dong and B. Liu, *J. Porous Mater.*, 2022, **29**, 1253–1263.
19 X. Xin, H. Shan, T. Tian, Y. Wang, D. Yuan, H. You and Y. Yao, *ACS Sustainable Chem. Eng.*, 2020, **8**, 13185–13194.
20 Z. Shi, Q. Su, T. Ying, X. Tan, L. Deng, L. Dong and W. Cheng, *J. CO2 Util.*, 2020, **39**, 101162.
21 Q. Su, Y. Qi, X. Yao, W. Cheng, L. Dong, S. Chen and S. Zhang, *Green Chem.*, 2018, **20**, 3232–3241.
22 D. M. Fernandes, A. F. Peixoto and C. Freire, *Dalton Trans.*, 2019, **48**, 13508–13528.
23 T. Zhang, J. Yin, Y. Pan, E. Liu, D. Liu and J. Meng, *Chem. Eng. J.*, 2020, **383**, 123166.
24 L. Deng, W. Sun, Z. Shi, W. Qian, Q. Su, L. Dong, H. He, Z. Li and W. Cheng, *J. Mol. Liq.*, 2020, **316**, 113883.
25 Y. Liu, Y. Wang, B. Jiang, L. Zheng, Z. Zhang, J. Liu and Z. Zhou, *ACS Sustainable Chem. Eng.*, 2023, **11**, 12366–12377.
26 S. Yue, H. Qu, X. Song, S. Zang and G. Deng, *Catal. Sci. Technol.*, 2021, **11**, 6999–7008.
27 Y. Liu, S. Li, Y. Chen, M. Li, Z. Chen, T. Hu, L. Shi, M. Pudukudy, S. Shan and Y. Zhi, *Chem. Eng. J.*, 2023, **474**, 145918.
28 T. Ying, X. Tan, Q. Su, W. Cheng, L. Dong and S. Zhang, *Green Chem.*, 2019, **21**, 2352–2361.
29 H. Peng, Q. Zhang, Y. Wang, H. Gao, N. Zhang, J. Zhou, L. Zhang, Q. Yang, Q. Yang and Z. Lu, *Appl. Catal., A*, 2022, **313**, 121463.
30 S. Pal, A. Mukherjee and P. Ghosh, *Mater. Today Sustain.*, 2021, **14**, 100082.
31 H. Du, Y. Ye, P. Xu and J. Sun, *J. CO2 Util.*, 2023, **67**, 102325.
32 Y. Ma, C. Chen, T. Wang, J. Zhang, J. Wu, X. Liu, T. Ren, L. Wang and J. Zhang, *Appl. Catal., A*, 2017, **547**, 265–273.
33 Y. Wang, Y. Liu, Q. Su, Y. Li, L. Deng, L. Dong, M. Fu, S. Liu and W. Cheng, *J. CO2 Util.*, 2022, **60**, 101976.
34 T. Wang, D. Zheng, J. Zhang, B. Fan, Y. Ma, T. Ren, L. Wang and J. Zhang, *ACS Sustainable Chem. Eng.*, 2018, **6**, 2574–2582.
35 T. Wang, Y. Ma, J. Jiang, X. Zhu, B. Fan, G. Yu, N. Li, S. Wang, T. Ren, L. Wang and J. Zhang, *J. Mol. Liq.*, 2019, **293**, 111479.
36 J. Zhang, X. Zhu, B. Fan, J. Guo, P. Ning, T. Ren, L. Wang and J. Zhang, *Mol. Catal.*, 2019, **466**, 37–45.
37 X. Zhu, J. Zhang, Z. Zhang, F. Liu, Y. Hu, Y. Liu, T. Ren, L. Wang and J. Zhang, *J. Mol. Liq.*, 2021, **328**, 115435.
38 D. Rocco, I. Chiarotto, F. D'Anna, L. Mattiello, F. Pandolfi, C. Rizzo and M. Feroci, *ChemElectroChem*, 2019, **6**, 4275–4283.
39 C. Rizzo, S. Marullo, M. Feroci, V. Accurso and F. D'Anna, *Dyes Pigm.*, 2021, **186**, 109035.
40 I. M. Gindri, D. A. Siddiqui, P. Bhardwaj, L. C. Rodriguez, K. L. Palmer, C. P. Frizzo, M. A. P. Martins and D. C. Rodrigues, *RSC Adv.*, 2014, **4**, 62594–62602.
41 M. Liu, L. Liang, T. Liang, X. Lin, L. Shi, F. Wang and J. Sun, *J. Mol. Catal. A: Chem.*, 2015, **408**, 242–249.
42 J. Chang, Y. Liu, Q. Su, L. Liu, L. Deng, T. Ying, L. Dong, Z. Luo, Q. Li and W. Cheng, *ChemistrySelect*, 2021, **6**, 6380–6387.

43 L. Guglielmero, A. Mezzetta, C. S. Pomelli, C. Chiappe and L. Guazzelli, *J. CO2 Util.*, 2019, **34**, 437–445.
44 W. Liao, H. Lin, M. Yin, J. Zhang, Z. Zhu and H. Lü, *Fuel*, 2022, **323**, 124389.
45 F. Norouzi and A. Abdolmaleki, *Fuel*, 2023, **334**, 126641.
46 H. Zhang, C. Meng, Q. Su, L. Dong, W. Liu, X. Wang, Y. Li and W. Cheng, *ChemistrySelect*, 2023, **8**, e202301015.
47 M. H. Anthofer, M. E. Wilhelm, M. Cokoja, M. Drees, W. A. Herrmann and F. E. Kühn, *ChemCatChem*, 2015, **7**, 94–98.
48 A. J. Kamphuis, F. Picchioni and P. P. Pescarmona, *Green Chem.*, 2019, **21**, 406–448.
49 F. Gao, C. Ji, S. Wang, J. Dong, C. Guo, Y. Gao and G. Chen, *Colloids Surf., A*, 2023, **666**, 131304.
50 L. Gao, Y. Zhou, Z. Li, J. He, Y. Qu, X. Zou, B. Liu, C. Ma, J. Sun and K. Guo, *J. CO2 Util.*, 2022, **65**, 102196.